POLITECNICO DI TORINO
Repository ISTITUZIONALE

Rotordynamic Coefficients for Labyrinth Gas Seals: Single Control Volume Model

*Original*
Rotordynamic Coefficients for Labyrinth Gas Seals: Single Control Volume Model / Malvano, R; Vatta, Furio; Vigliani, Alessandro. - In: MECCANICA. - ISSN 0025-6455. - 36 (6):(2001), pp. 731-744. [10.1023/A:1016369408324]

*Availability:*
This version is available at: 11583/1406804 since:

*Publisher:*

*Published*
DOI:10.1023/A:1016369408324

*Terms of use:*

This article is made available under terms and conditions as specified in the corresponding bibliographic description in the repository

*Publisher copyright*

(Article begins on next page)

24 January 2025

Post print (i.e. final draft post-refereeing) version of an article published on *Meccanica*. Beyond the journal formatting, please note that there could be minor changes from this document to the final published version. The final published version is accessible from here:
http://dx.doi.org/10.1023/A:1016369408324
This document has made accessible through PORTO, the Open Access Repository of Politecnico di Torino (http://porto.polito.it), in compliance with the Publisher's copyright policy as reported in the SHERPA-ROMEO website:
http://www.sherpa.ac.uk/romeo/issn/0025-6455/

# Rotordynamic coefficients for labyrinth gas seals: single control volume model

R. Malvano[a], F. Vatta[b], A. Vigliani[b]

[a]C.N.R. – Centro Studi Dinamica Fluidi
C.so Duca degli Abruzzi, 24 - 10129 Torino - ITALY

[b]Dipartimento di Meccanica - Politecnico di Torino
C.so Duca degli Abruzzi, 24 - 10129 Torino - ITALY
E-mail: *alessandro.vigliani@polito.it*

**Keywords** tribology; labyrinth seals; rotordynamic coefficients

**Abstract** *A numerical code has been developed to determine the rotordynamic coefficients of straight-through labyrinth gas seals in the case of a single volume model. Some considerations are drawn concerning the position of the sonic section when the flow is choked. Furthermore the influence of kinematic viscosity varying with pressure has been considered. The results are compared with the experimental and theoretical ones available in the literature. The agreement between results is fairly good.*

## Nomenclature

| | | | |
|---|---|---|---|
| $A_i$ | cavity transverse area | $N_t$ | number of seal strips |
| $a$, $b$ | radial seal displacement components due to elliptical whirl | $p$ | pressure |
| | | $p_r$ | reservoir pressure |
| $a_r$, $a_s$ | dimensionless length | $p_s$ | sump pressure |
| $B_i$ | cavity height | $R$ | gas constant |
| $C$ | direct damping coefficient | $R_s$ | seal radius |
| $c$ | cross–coupled damping coefficient | $S_r$ | wet perimeter on rotor |
| $D_i$ | hydraulic diameter | $S_s$ | wet perimeter on stator |
| $H_i$ | radial clearance | $T$ | absolute temperature |
| $i$ | $i-$ th section ; $i = 0 =$ inlet; $i = N_t =$ outlet | $t$ | time |
| | | $U_i$ | tangential velocity |
| $K$ | direct stiffness coefficient | $U_0/(\omega R_s)$ | inlet velocity ratio |
| $k$ | cross–coupled stiffness coefficient | $\alpha$ | cavity geometric coefficient |
| $L_i$ | cavity length | $\gamma$ | specific heats ratio |
| $L_T$ | labyrinth seal total length | $\vartheta$ | angular displacement |
| $M$ | Mach number | $\lambda$ | exponent in the kinematic viscosity-pressure relationship |
| $\dot{m}$ | leakage mass flow rate per unit circumference | $\mu_i$ | flow coefficient |
| $m_r$, $n_r$ | coefficients for Blasius relation (rotor) | $\mu_g$ | kinetic energy carryover coefficient |
| | | $\nu$ | kinematic viscosity |
| $m_s$, $n_s$ | coefficients for Blasius relation (stator) | $\rho$ | fluid density |
| | | $\tau_r$, $\tau_s$ | shear stress on rotor, stator |
| $N_c$ | number of labyrinth cavities | $\omega$ | rotor angular speed |

# 1 Introduction

Self–excited vibrations represent a serious problem in turbomachinery: they arise in the form of shaft sub–synchronous precession, i.e. at angular speed lower than that of the shaft itself.
The forces that determine such motion have different origins; one of these is due to the labyrinth seals that are commonly used to reduce fluid leakage from high pressure regions to low pressure ones. Basically their working principle lies in accelerating and successively decelerating a compressible flow, leading to dissipation of kinetic energy due to viscous friction. It is then evident the importance of studying the dynamic characteristics of labyrinth seals: as a matter of fact they can effectively influence the motor performances.
Labyrinth seals can possess different geometry; in the present paper, we will consider the simplest geometries, known as *straight-through labyrinth seal*. In this case, the geometrical parameters of the cavity ($A_i$, $B_i$, $H_i$ and $L_i$) are constant along the seal.
In this field the literature is vast. It is worth noting that Black (1) was the first to describe an annular seal behavior through dynamic coefficients, in analogy with the studies on lubricated bearings.
The analysis to determine such coefficients is based on the following models:
• single control volume
• multiple control volume.
The aim of the present work is to develop a numerical code to determine stiffness and damping coefficients for a labyrinth seal when adopting a single control volume model.
Moreover the authors will prove that, in the case of sonic flow, the sonic condition can be placed only in correspondence of the outlet section. Furthermore the work focuses on the influence of the hypothesis of kinematic viscosity varying with pressure.
To the best of the author's knowledge, these findings do not appear to have been reported previously in literature.
Finally, in order to test the reliability of the code, the authors compare their results with the experimental work of Benckert and Wachter (2) in the case of non rotating shaft and with numerical results obtained by Scharrer (3).

# 2 Mathematical model

In the following section we summarize results already present in the literature, relative to the case of a single control volume (4). With reference to Fig. 1, showing a generic cavity of a labyrinth seal, the continuity equation for the control volume under analysis is given by:

$$\frac{\partial}{\partial t}\left(\rho_i A_i\right) + \frac{\partial}{\partial \vartheta}\left(\frac{\rho_i U_i A_i}{R_s}\right) + \dot{m}_{i+1} - \dot{m}_i = 0 \tag{1}$$

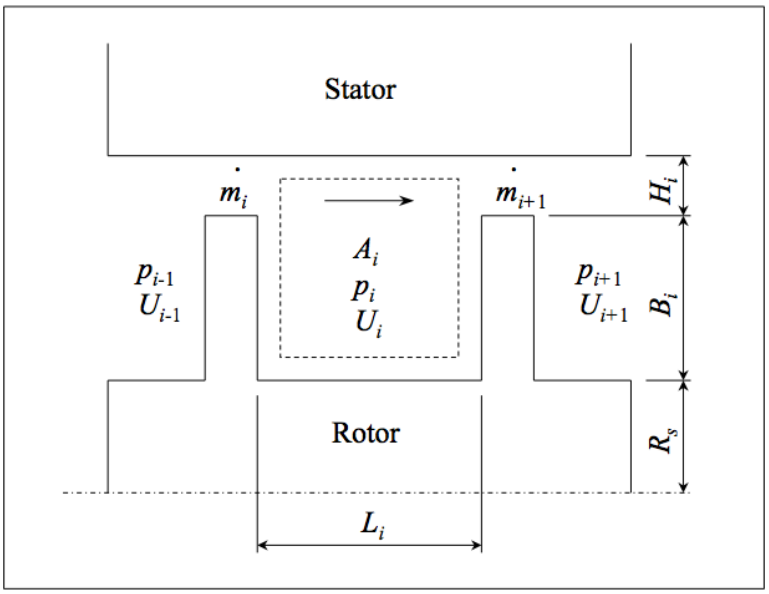


Figure 1: Cavity geometry

while the momentum equation is:

$$\frac{\partial}{\partial t}\left(U_i \rho_i A_i\right) + \frac{\partial}{\partial \vartheta}\left(\frac{\rho_i U_i^2 A_i}{R_s}\right) + U_i \dot{m}_{i+1} - U_{i-1}\dot{m}_i = -\frac{A_i}{R_s}\frac{\partial p_i}{\partial \vartheta} + \left(\tau_{r_i} a_{r_i} - \tau_{s_i} a_{s_i}\right) L_i \tag{2}$$

where

$$a_{r_i} = \frac{S_{r_i}}{L_i} \qquad \text{and} \qquad a_{s_i} = \frac{S_{s_i}}{L_i}.$$

Shear stresses are described by Blasius model, valid for turbulent flows in smooth pipes. It holds:

$$\tau_{s_i} = \frac{1}{2}\rho_i U_i^2 n_s \left[\frac{|U_i|\ D_i}{\nu}\right]^{m_s} \text{sign}\left(U_i\right) \tag{3}$$

$$\tau_{r_i} = \frac{1}{2}\rho_i \left(\omega R_s - U_i\right)^2 n_r \left[\frac{|\omega R_s - U_i|\ D_i}{\nu}\right]^{m_r} \text{sign}\left(\omega R_s - U_i\right) \tag{4}$$

where $D_i = 2(B_i + H_i)L_i/(B_i + H_i + L_i)$
For a subsonic flow, the flow rate $\dot{m}$, according to Neumann's empirical formula (5), is given by:

$$\dot{m}_i = \mu_g \mu_i H_i \sqrt{\frac{p_{i-1}^2 - p_i^2}{RT}} \tag{5}$$

where $\mu_i$ is the *flow coefficient*, while $\mu_g$ is the *kinetic energy carryover coefficient*, given by the following empirical expressions:

$$\mu_i = \frac{\pi}{\pi + 2 - 5\beta_i + 2\beta_i^2} \qquad \text{where} \qquad \beta_i = \left(\frac{p_{i-1}}{p_i}\right)^{\frac{\gamma-1}{\gamma}} - 1$$

$$\mu_g = \sqrt{\frac{N_t}{(1-\alpha)N_t + \alpha}} \qquad \text{where} \qquad \alpha = 1 - \left(1 + 16,6\frac{H_i}{L_i}\right)^{-2}$$

When the flow is choked (i.e. the outlet section is sonic, as proved in Section 3), the flow rate, according to Fliegner's (6), becomes:

$$\dot{m}_{N_t} = 0,51 \mu_g p_{N_c} \frac{H_i}{\sqrt{RT}} \tag{6}$$

The following hypotheses hold:

- the flow thermodynamic evolution follows the ideal gas law
- temperature is constant along the seal
- the axial component of velocity can be neglected when computing shear stresses.

It is now possible to determine the pressure and the speed in each cavity by substituting expressions (3÷6) in eqs. (1) and (2).
The solution of the of the problem can be obtained by means of perturbation technique; let

$$p_i = p_{i,0} + p_i^{'} \qquad H_i = H_{i,0} + H_i^{'} = H_0 + H^{'}$$

$$U_i = U_{i,0} + U_i^{'} \qquad A_i = A_{i,0} + L_i\, H_i^{'} = A_0 + L\, H^{'}$$

where subscript 0 represents static components (zeroth order), that are constant inside each cavity but vary from cavity to cavity, while superscript $'$ stands for variable components (first order), that are due to a perturbation (displacement) of the rotor from its centered position.
The first order terms are functions both of angular displacement and of time, and are responsible for the forces exerted on the rotor. With respect to zeroth order, it holds:

$$\dot{m}_i = \dot{m}_{i+1} = \dot{m}_0 \tag{7}$$

$$\dot{m}_0\ (U_{i,0} - U_{i-1,0})\ -\ L\ \left(a_{r_i}\,\tau_{r_{i,0}}\ -\ a_{s_i}\,\tau_{s_{i,0}}\right) = 0 \tag{8}$$

Given inlet and outlet pressures, by means of eq. (7) it is possible to compute the pressure distribution along the seal and the flow rate $\dot{m}_0$; this result is obtained adopting an iterative technique and verifying whether the flow is choked or not in correspondence of the outlet section. Finally, the tangential velocity distribution can be determined through eq. (8).
When considering the first order terms, we have:

$$\begin{cases} G_{2i}\dfrac{\partial H^{'}}{\partial t} + G_{1i}\dfrac{\partial p_i^{'}}{\partial t} + G_{2i}\dfrac{U_{i,0}}{R_s}\dfrac{\partial H^{'}}{\partial \vartheta} + G_{1i}\dfrac{U_{i,0}}{R_s}\dfrac{\partial p_i^{'}}{\partial \vartheta} + G_{1i}\dfrac{p_{i,0}}{R_s}\dfrac{\partial U_i^{'}}{\partial \vartheta} + G_{3i}\,p_i^{'} + \\ + G_{4i}\,p_{i-1}^{'} + G_{5i}\,p_{i+1}^{'} = 0 \\ X_{1i}\dfrac{\partial U_i^{'}}{\partial t} + X_{1i}\dfrac{U_{i,0}}{R_s}\dfrac{\partial U_i^{'}}{\partial \vartheta} + \dfrac{A_{i,0}}{R_s}\dfrac{\partial p_i^{'}}{\partial \vartheta} + X_{2i}\,U_i^{'} - \dot{m}_0\,U_{i-1}^{'} + X_{3i}\,p_i^{'} + \\ + X_{4i}\,p_{i-1}^{'} + X_{5i}\,H^{'} = 0 \end{cases} \tag{9}$$

where coefficients $G_{1i}$, $G_{2i}$, $G_{3i}$, $G_{4i}$, $G_{5i}$, and $X_{1i}$, $X_{2i}$, $X_{3i}$, $X_{4i}$, $X_{5i}$ are functions of zeroth order variables. Their expressions are given in Appendix A.
Assuming the shaft perturbation to be an elliptical orbit of semi–axes $a$ and $b$, it yields:

$$H^{'} = -\frac{a}{2}\left[\cos(\vartheta - \omega\,t) + \cos(\vartheta + \omega\,t)\right] - \frac{b}{2}\left[\cos(\vartheta - \omega\,t) - \cos(\vartheta + \omega\,t)\right] \tag{10}$$

Consequently the pressure and velocity fluctuations are assumed to be in the format:

$$\begin{cases} p_i^{'} &= p_i^{+\,c}\cos(\vartheta + \omega\,t) + p_i^{+\,s}\sin(\vartheta + \omega\,t) + p_i^{-\,c}\cos(\vartheta - \omega\,t) + \\ &\quad + p_i^{-\,s}\sin(\vartheta - \omega\,t) \\ U_i^{'} &= U_i^{+\,c}\cos(\vartheta + \omega\,t) + U_i^{+\,s}\sin(\vartheta + \omega\,t) + U_i^{-\,c}\cos(\vartheta - \omega\,t) + \\ &\quad + U_i^{-\,s}\sin(\vartheta - \omega\,t) \end{cases} \tag{11}$$

Substituting eqs. (10) and (11) into (9) and grouping like terms of sines and cosines eliminates the time and angular displacement dependency; it yields eight independent linear algebraic equations per cavity, in the following unknowns: $p_i^{+\,c}$ $p_i^{+\,s}$ $p_i^{-\,c}$ $p_i^{-\,s}$ $U_i^{+\,c}$ $U_i^{+\,s}$ $U_i^{-\,c}$ $U_i^{-\,s}$.
The resulting system for cavity $i$ besides the above unknowns, depends on the same unknowns expressed as functions of cavity $i+1$ and $i-1$; hence it is a *block-tridiagonal system* that can be easily solved.

Being the system linear, the unknowns represented by the amplitudes of expressions (11) are determined by superimposition of the known terms; in particular, for pressures it yields:

$$p_i^{+\,s} = a\,F_{ai}^{+\,s} + b\,F_{bi}^{+\,s} \qquad p_i^{-\,s} = a\,F_{ai}^{-\,s} + b\,F_{bi}^{-\,s}$$

$$p_i^{+\,c} = a\,F_{ai}^{+\,c} + b\,F_{bi}^{+\,c} \qquad p_i^{-\,c} = a\,F_{ai}^{-\,c} + b\,F_{bi}^{-\,c}$$

where subscript $a$ refers to the pressure component obtained when letting the conditions $a = 1$ and $b = 0$ in eq. (10), while subscript $b$ refers to the pressure component obtained when letting the conditions $a = 0$ and $b = 1$ in eq. (10).
By means of the technique proposed by Scharrer, the stiffness and damping coefficients can be computed as follows:

$$K = \pi\,R_s \sum_{i=1}^{N_c} \left(F_{ai}^{+\,c} + F_{ai}^{-\,c}\right) L \qquad k = \pi\,R_s \sum_{i=1}^{N_c} \left(F_{bi}^{+\,s} - F_{bi}^{-\,s}\right) L$$

$$C = \frac{-\pi R_s}{\omega} \sum_{i=1}^{N_c} \left(F_{ai}^{+\,s} - F_{ai}^{-\,s}\right) L \qquad c = \frac{\pi R_s}{\omega} \sum_{i=1}^{N_c} \left(F_{bi}^{+\,c} + F_{bi}^{-\,c}\right) L$$

# 3 Sonic conditions

The fluid motion inside the seal in axial direction can be assumed to behave as the "nearly unidimensional" flow of a compressible fluid in a pipe of constant section $A_F$. The term "nearly unidimensional" we refer to the condition of physical and kinematic quantities varying only axially, being constant across the section.
With reference to the internal flow theory (7), it is possible to assume the Mach number relative variation due to three terms; it yields:

$$\begin{aligned} \frac{dM^2}{M^2} &= -\frac{2}{1-M^2}\left(1+\frac{\gamma-1}{2}M^2\right)\frac{dA_F}{A_F} + \frac{M^2}{1-M^2}\gamma\left(1+\frac{\gamma-1}{2}M^2\right)dF + \\ &+ \frac{1+\gamma M^2}{1-M^2}M^2\left(1+\frac{\gamma-1}{2}M^2\right)\frac{dT^0}{T^0} \end{aligned} \tag{12}$$

where $F$ is a function taking into account the friction and drag effects and $T^0$ is the total temperature. Through the above equation it is possible to analyze the flow in the seal and to prove that, if there is a sonic section, it can only be the outlet section of the seal itself. In the case under examination, $dA_F$ is null, as well as $dT^0$ is null under the hypothesis of adiabatic flow. Consequently it holds:

$$dM^2 = \frac{\gamma M^4\left(1+\frac{\gamma-1}{2}M^2\right)}{1-M^2}dF \tag{13}$$

The numerator of eq. (13) is always positive along the axial direction; hence the sign of $dM$ depends on the value of $M$ with respect to one. If we suppose that $M < 1$ at the inlet section, eq. (13) gives a positive value for $dM$, hence $M$ grows along axial direction. This growth can not lead to $M = 1$ in a section inside the seal, because two different conditions could take place immediately downstream this hypothetical section, but either of them is contradicted by eq. (13):

- $M$ can not grow (i.e. $dM > 0$), for, from eq. (13), $dM$ is negative if $M > 1$;
- $M$ can not decrease (i.e. $dM < 0$), for, from eq. (13), $dM$ is positive if $M < 1$.

Hence,depending on pressures upstream and downstream the labyrinth seal, only the following two conditions can take place:

- the flow is subsonic along the whole seal;
- the flow becomes sonic at the outlet section of the seal and then, externally to the seal itself, it suits to downstream pressure through a shock wave; it is the case of chocked flow.

These results hold for adiabatic flows, while the analytical models derived by Iwatsubo, Childs and Scharrer consider an isothermic flow, so that the leakage flow rate can be expresses as in eq. (5). Hence it is interesting to investigate the consequences determined by the two different approaches. Total temperature $T^0$ depends on static temperature $T$ according to the following expression:

$$T^0 = T\left(1 + \frac{\gamma - 1}{2} M^2\right)$$

Hence, eq. (12), in the isothermic case, becomes:

$$\begin{aligned} \left(1 - M^2\right) &= \gamma M^4 \left(1 + \frac{\gamma - 1}{2} M^2\right) dF + \\ &+ M^2 \left(1 + \gamma M^2\right) \left(1 + \frac{\gamma - 1}{2} M^2\right) \frac{T}{T^0} \frac{\gamma - 1}{2} dM^2 \end{aligned} \tag{14}$$

After a few simple passages, it yields:

$$-dM^2 \left[\frac{(\gamma - 1)\,\gamma}{2} M^4 + \frac{\gamma + 11}{2} M^2 - 1\right] = \gamma M^4 \left(1 + \frac{\gamma - 1}{2} M^2\right) dF \tag{15}$$

The roots of the left hand side of eq. (15) are:

$$M_1^2 = \frac{1}{\gamma} \qquad M_2^2 = -\frac{2}{\gamma - 1}$$

so eq. (15) can be written as:

$$dM^2 = \frac{\gamma M^4 \left(1 + \frac{\gamma - 1}{2} M^2\right) dF}{\left(\frac{1}{\gamma} - M^2\right)\left(M^2 + \frac{2}{\gamma - 1}\right)} \tag{16}$$

It can be immediately seen that the limit value that the Mach number can reach at the outlet section of the seal differs from unity, and is given by:

$$M = \gamma^{-\frac{1}{2}}$$

Therefore, in the isothermic case, the Mach number grows along the seal, however without reaching the sonic condition: hence the flow is always subsonic.

# 4 Influence of pressure on kinematic viscosity

It si well known that kinematic viscosity is strongly influenced by pressure when pressure itself undergoes significant variations. High pressure ratios (of order 20 or even 30) between inlet and outlet may take place in turbomachinery. In these conditions the assumption that kinematic viscosity is independent of pressure does not hold. Consequently, by means of a perturbative technique, from eq. (3) it holds:

$$\tau_{s_i} = \tau_{s_{i,0}} + \left(\frac{\partial \tau_{s_i}}{\partial U_i}\right)_0 U_i^{'} + \left(\frac{\partial \tau_{s_i}}{\partial D_i} \cdot \frac{\partial D_i}{\partial H_i}\right)_0 H_i^{'} + \left(\frac{\partial \tau_{s_i}}{\partial \rho_i}\right)_0 \rho_i^{'} \tag{17}$$

In the most general case, the relationship between viscosity $\nu$ and pressure is $\nu/\nu_0 = (p/p_0)^{-\lambda}$, having supposed constant temperature along the seal.
Last term of the right hand side of eq. (17) becomes:

$$\left(\frac{\partial \tau_{s_i}}{\partial \rho_i}\right)_0 \rho_i' = \left[\frac{\tau_{s_i}}{\rho_i}\left(1 + m_s \lambda\right)\right]_0 \frac{p_i'}{RT} = \tau_{s_{i,0}} \frac{1 + m_s \lambda}{p_{i,0}} p_i'$$

Let $\tau_{s_i}$ be

$$\tau_{s_i} = \tau_{s_{i,0}} + O_s(1)$$

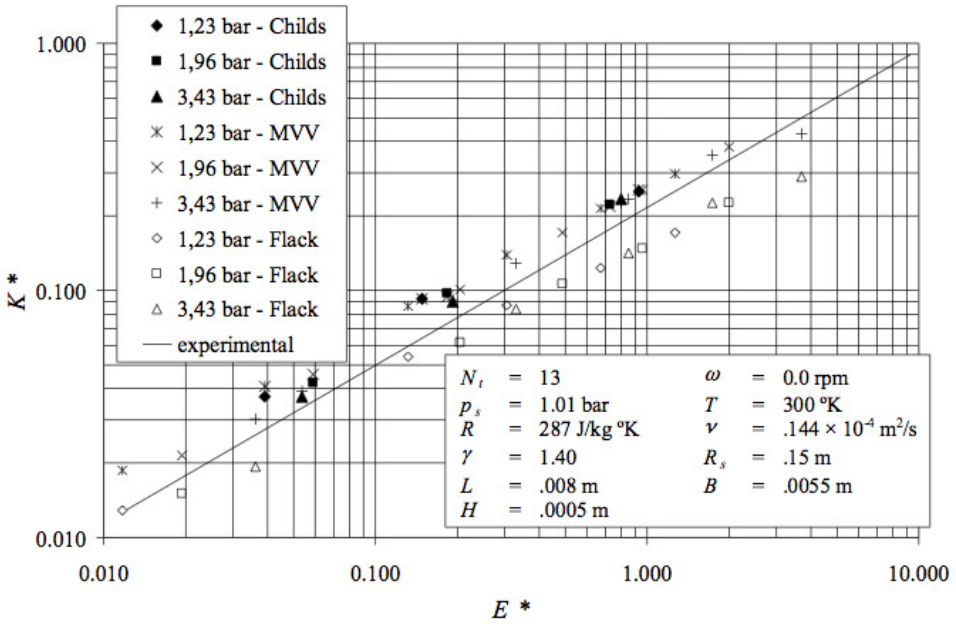


Figure 2: Comparison of results $\left(k^{\star} = \dfrac{H_i k}{R_s L_i N_c \left(p_r - p_s\right)},\ \ E^{\star} = \dfrac{.5\rho_0 U_0^2}{p_r - p_s}\right)$

where

$$O_s(1) = \tau_{s_{i,0}} \left[ \frac{2 + m_s}{U_{i,0}} U_i' + \frac{m_s D_i}{2\left(B + H\right)^2} H' + \frac{1 + m_s \lambda}{p_{i,0}} p_i' \right]$$

Likewise, from eq. (4) we have:

$$\tau_{r_i} = \tau_{r_{i,0}} + O_r(1)$$

where:

$$O_r(1) = \tau_{r_{i,0}} \left[ -\frac{2 + m_r}{\omega R_s - U_{i,0}} U_i' + \frac{m_r D_i}{2\left(B + H\right)^2} H' + \frac{1 + m_r \lambda}{p_{i,0}} p_i' \right]$$

Hence the effect of viscosity varying with pressure affects only term $X_{3i}$ (see Appendix A). When dependence of kinematic viscosity on pressure may be neglected (i.e. $\lambda = 0$), the above equations coincide with expressions derived by Childs (4).

# 5 Numerical results and conclusions

A computational code was developed to determine the dynamic coefficients of labyrinth seals. We considered a single control volume model and tested the code comparing our results, identified by the acronym MVV, with those obtained by other researchers. All the seal under examination are teeth on stator (T.O.S.) seals.
Firstly we compare our results with those published by Benckert e Wachter (2): they appear to be in good agreement, as it can be seen in Fig. 2. This figure shows also the results published by Childs and Scharrer (4) and by Williams and Flack (8).
Figures $3 \div 6$ show the comparison between our results and those from Scharrer (3) for all the dynamic coefficients.
The effects of variable kinematic viscosity $\nu$ are depicted in figures $7 \div 10$, where we plot the dynamic coefficients versus $\omega$ both in the case of $\nu = \text{const}$ and of $\nu = f(p)$. These plots show that direct stiffness and cross–coupled damping coefficients are not affected by viscosity variations; moreover, for low pressure ratios, changes of viscosity have negligible influence also on cross–coupled stiffness and direct damping coefficients. With growing pressure ratio, kinematic viscosity undergoes relevant variations and hence it influences significantly the dynamic coefficients with growing shaft velocity $\omega$.

Finally, it is worth noting that the coefficients $n$ and $m$ used to compute the shear stresses hold for smooth pipes; as a matter of fact, real surfaces are rough, hence these coefficients should be suitably adjusted. We verified that their numerical values play a fundamental role in evaluating the dynamic coefficients: in fact, even a slight change causes strong variations of dynamic coefficient.

# References


[1] Black H. F., Jenssen D. N., *Dynamic Hybrid Bearing Characteristics of Annular Controlled Leakage Seals*, Proc. Inst. Mech. Eng, **184**, pp.92–100, 1970.

[2] Benckert H., Wachter J., *Flow Induced Spring Coefficients of Labyrinth Seals for Applications in Rotor Dynamics*, NACA CP 2133, pp.189–212, 1980.

[3] Scharrer J. K., *A Comparison of Experimental and Theoretical Results for Rotordynamic Coefficients for Labyrinth Gas Seals*, TRC Report No. SEAL-2-85, Texas A&M University, 1985.

[4] Childs D. W., Scharrer J. K., *An Iwatsubo–based Solution for Labyrinth Seals: Comparison to Experimental Results*, J. Eng. Gas Turbines and Power, **108**, pp.325–331, 1986.

[5] Neumann K., *Zur Frage der Verwendung von Durchblickdichtungen im Dampfturbinenbau*, Maschinentechnik, **13** (4), 1964.

[6] John E. A. J., *Gas Dynamics*, Wiley, 1979.

[7] Shapiro A. H., *The Dynamics and Thermodynamics of Compressible Fluid Flow*, vol. 1, Wiley, p.230, 1954.

[8] Williams B. P., Flack, R. D., *Calculation of Rotor Dynamic Coefficients for Labyrinth Seals*, Proc. 7th Congress ISROMAC, Vol.A, Honolulu, pp.871–880, 1998.

# Appendix A

Definition of the first order continuity and momentum equation coefficients:

$$G_{1i} = \frac{A_{i,0}}{RT}$$

$$G_{2i} = \frac{p_{i,0}\, L_i}{RT}$$

$$G_{3i} = \dot{m}_0 \left\{ \frac{p_{i,0}}{p_{i-1,0}^2 - p_{i,0}^2} + \frac{p_{i,0}}{p_{i,0}^2 - p_{i+1,0}^2} + \mu_{i,0} \frac{5 - 4\,\beta_{i,0}}{\pi} \cdot \frac{\gamma - 1}{\gamma} \cdot \frac{1}{p_{i,0}} \left( \frac{p_{i-1}}{p_i} \right)_0^{\frac{\gamma-1}{\gamma}} + \right.$$

$$\left. + \mu_{i+1,0} \frac{5 - 4\,\beta_{i+1,0}}{\pi} \cdot \frac{\gamma - 1}{\gamma} \cdot \frac{1}{p_{i+1,0}} \left( \frac{p_i}{p_{i+1}} \right)_0^{-\frac{1}{\gamma}} \right\}$$

$$G_{4i} = -\dot{m}_0 \left[ \frac{p_{i-1,0}}{p_{i-1,0}^2 - p_{i,0}^2} + \mu_{i,0} \frac{5 - 4\,\beta_{i,0}}{\pi} \cdot \frac{\gamma - 1}{\gamma} \cdot \frac{1}{p_{i,0}} \left( \frac{p_{i-1}}{p_i} \right)_0^{-\frac{1}{\gamma}} \right]$$

$$G_{5i} = -\dot{m}_0 \left[ \frac{p_{i+1,0}}{p_{i,0}^2 - p_{i+1,0}^2} + \mu_{i+1,0} \frac{5 - 4\,\beta_{i+1,0}}{\pi} \cdot \frac{\gamma - 1}{\gamma} \cdot \frac{1}{p_{i+1,0}} \left( \frac{p_i}{p_{i+1}} \right)_0^{\frac{\gamma-1}{\gamma}} \right]$$

$$X_{1i} = \frac{p_{i,0}\, A_{i,0}}{RT}$$

$$X_{2i} = \dot{m}_0 + \frac{2 + m_s}{U_{i,0}} L_i\, a_{s_i}\, \tau_{s_{i,0}} + \frac{2 + m_r}{\omega R_s - U_{i,0}} L_i\, a_{r_i}\, \tau_{r_{i,0}}$$

$$X_{3i} = -\dot{m}_0\, (U_{i,0} - U_{i-1,0}) \left[ \frac{p_{i,0}}{p_{i-1,0}^2 - p_{i,0}^2} + \mu_{i,0} \frac{5 - 4\,\beta_{i,0}}{\pi} \cdot \frac{\gamma - 1}{\gamma} \cdot \frac{1}{p_{i,0}} \left( \frac{p_{i-1}}{p_i} \right)_0^{\frac{\gamma-1}{\gamma}} \right] +$$

$$+ \frac{1 + m_s \lambda}{p_{i,0}} L_i\, a_{s_i}\, \tau_{s_{i,0}} - \frac{1 + m_r \lambda}{p_{i,0}} L_i\, a_{r_i}\, \tau_{r_{i,0}}$$

$$X_{4i} = \dot{m}_0\, (U_{i,0} - U_{i-1,0}) \left[ \frac{p_{i-1,0}}{p_{i-1,0}^2 - p_{i,0}^2} + \mu_{i,0} \frac{5 - 4\,\beta_{i,0}}{\pi} \cdot \frac{\gamma - 1}{\gamma} \cdot \frac{1}{p_{i,0}} \left( \frac{p_{i-1}}{p_i} \right)_0^{-\frac{1}{\gamma}} \right]$$

$$X_{5i} = \frac{\dot{m}_0}{H_0}\, (U_{i,0} - U_{i-1,0}) + \frac{m_s\, D}{2\,(B + H)^2} L_i\, a_{s_i}\, \tau_{s_{i,0}} - \frac{m_r\, D}{2\,(B + H)^2} L_i\, a_{r_i}\, \tau_{r_{i,0}}$$

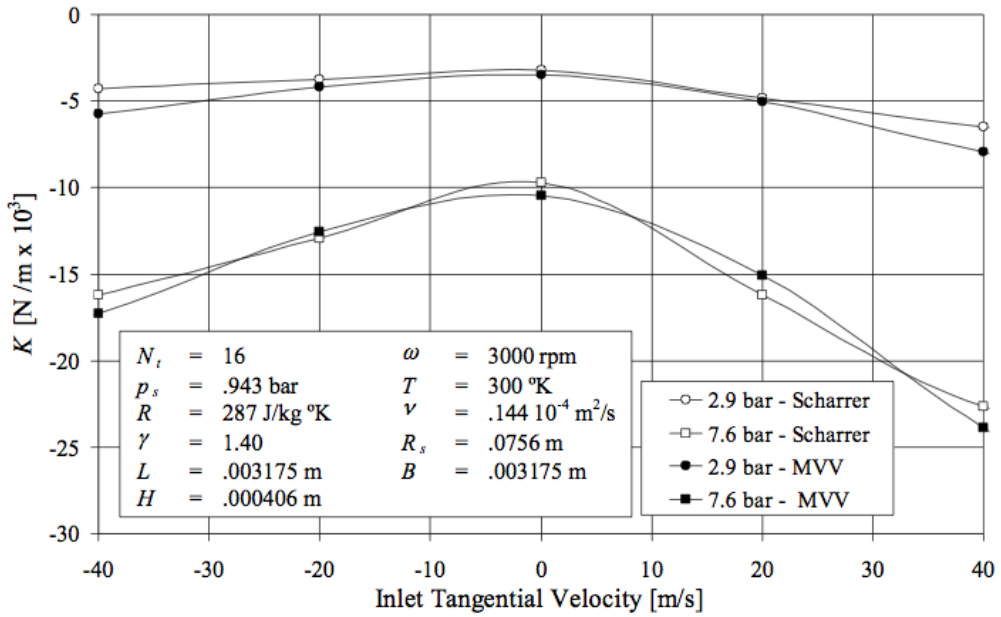


Figure 3: Direct stiffness coefficient versus inlet tangential velocity

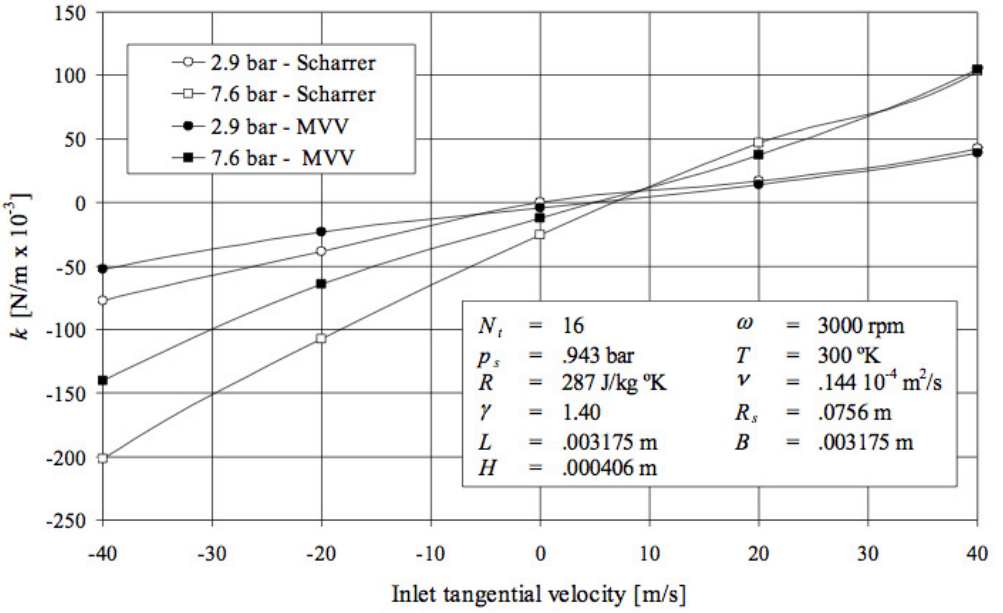


Figure 4: Cross–coupled stiffness coefficient versus inlet tangential velocity

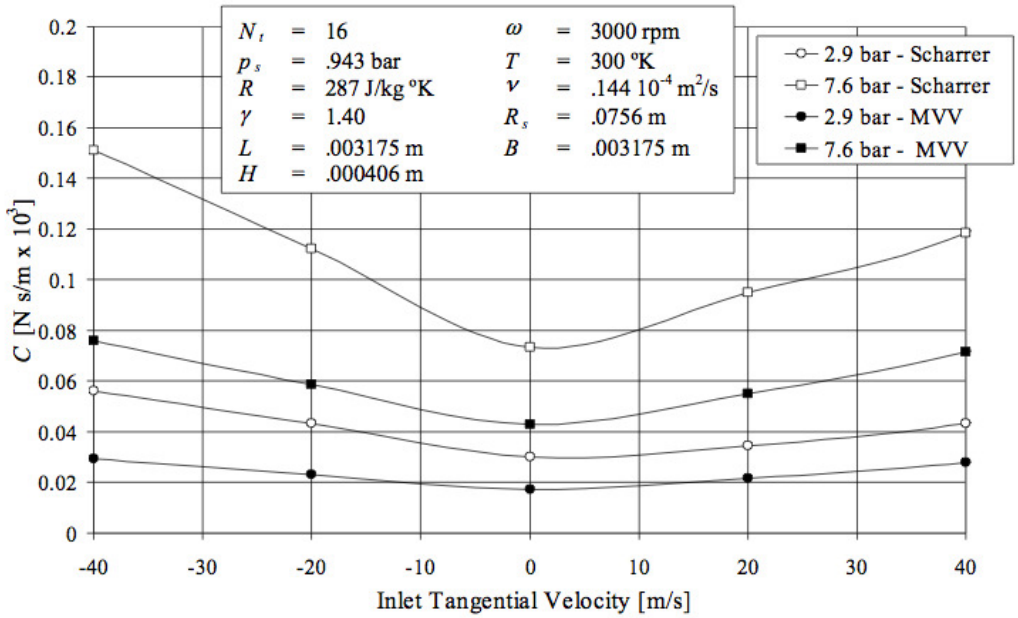


Figure 5: Direct damping coefficient versus inlet tangential velocity

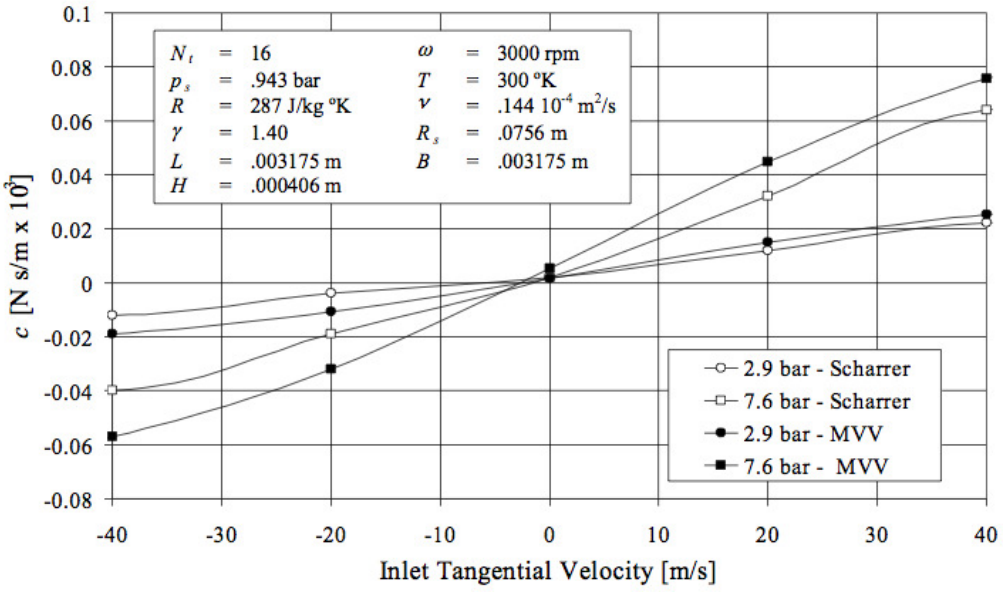


Figure 6: Cross-coupled damping coefficient versus inlet tangential velocity

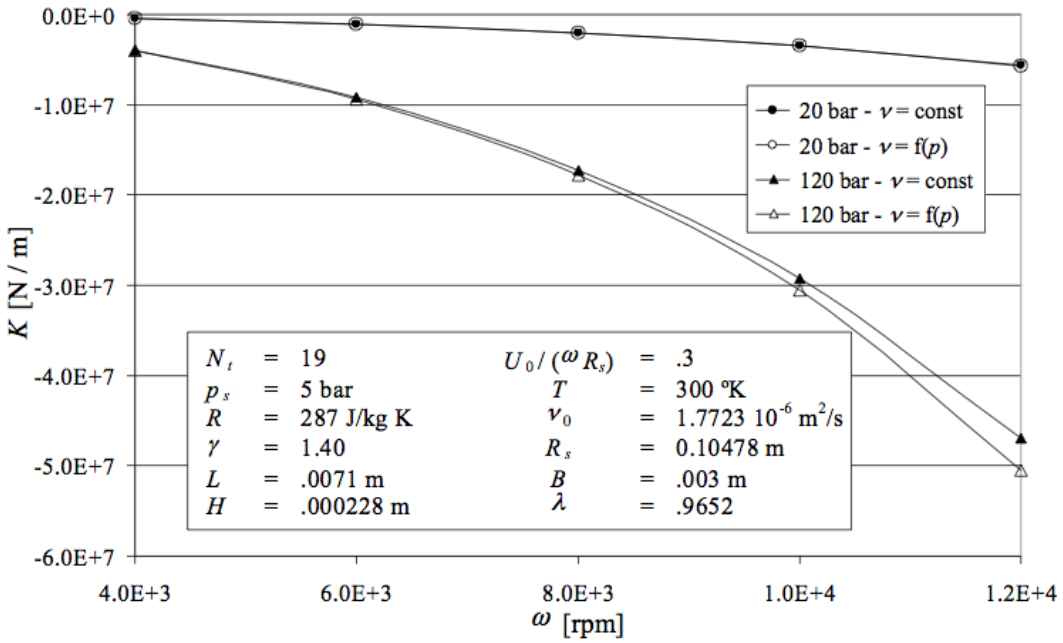


Figure 7: Direct stiffness coefficient versus rotor angular speed

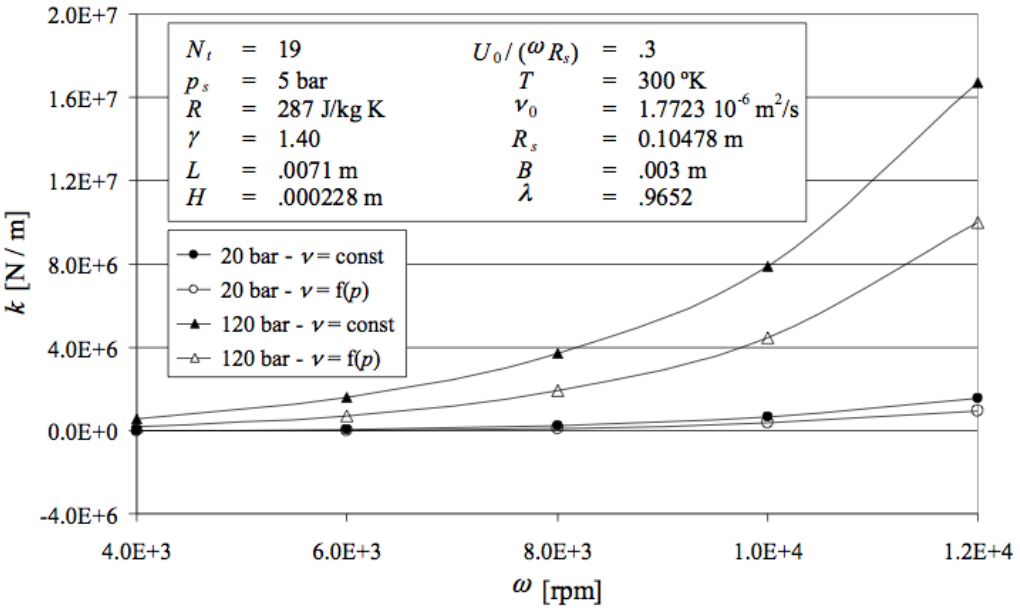


Figure 8: Cross-coupled stiffness coefficient versus rotor angular speed

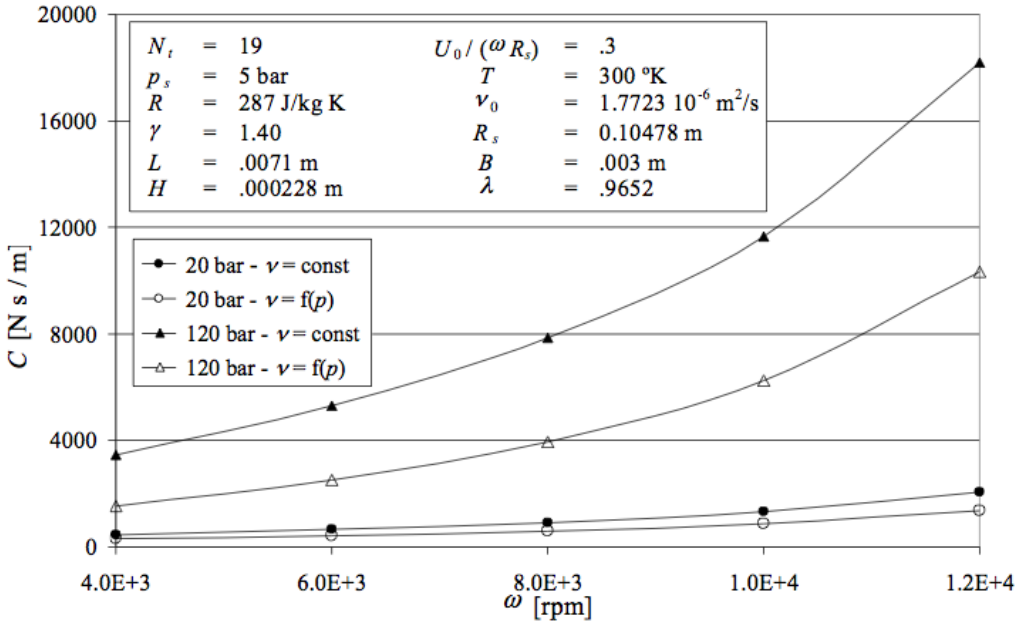


Figure 9: Direct damping coefficient versus rotor angular speed

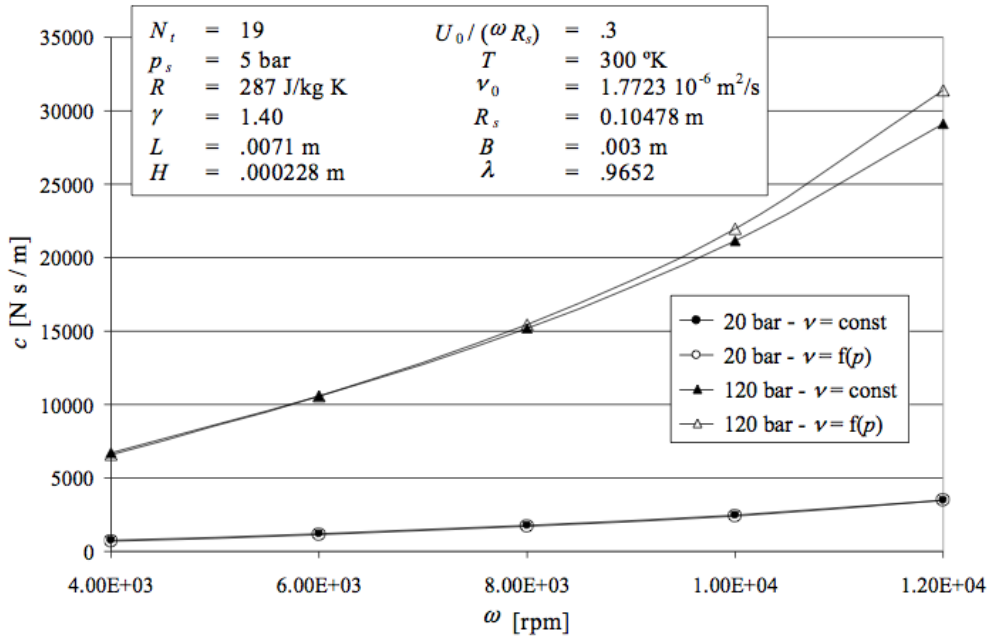


Figure 10: Cross-coupled damping coefficient versus rotor angular speed